

See discussions, stats, and author profiles for this publication at: <https://www.researchgate.net/publication/234847974>

Ab initio molecular dynamics study of polarization effects on ionic hydration in aqueous AlCl_3 solution

ARTICLE *in* THE JOURNAL OF CHEMICAL PHYSICS · DECEMBER 2003

Impact Factor: 2.95 · DOI: 10.1063/1.1627323

CITATIONS

29

READS

13

3 AUTHORS, INCLUDING:



Takaumi Kimura

Japan Atomic Energy Agency

202 PUBLICATIONS 2,556 CITATIONS

SEE PROFILE

COMMUNICATIONS

Exploring the Opsin shift with <i>ab initio</i> methods: Geometry and counterion effects on the electronic spectrum of retinal	
Marko Schreiber, Volker Buß, and Minoru Sugihara.	12045
Reduction of the hydrophobic attraction between charged solutes in water	
J. Dzubiella and J.-P. Hansen.	12049
Enhanced hydrolysis at monolayer MgO films	
L. Savio, E. Celasco, L. Vattuone, and M. Rocca.	12053

ARTICLES

Theoretical Methods and Algorithms

Quantum dynamics scattering study of AB+CDE reactions: A seven-dimensional treatment for the $H_2 + C_2H$ reaction	
Dunyou Wang.	12057
A new approach to calculating the memory kernel of the generalized quantum master equation for an arbitrary system–bath coupling	
Qiang Shi and Eitan Geva.	12063
Recovery of the Smoluchowski–Collins–Kimball kinetics parameters from fluorescence quenching decays	
Jacek Kłos and Andrzej Molski.	12077
Absolute entropy and free energy of fluids using the hypothetical scanning method.	
I. Calculation of transition probabilities from local grand canonical partition functions	
Agnieszka Szarecka, Ronald P. White, and Hagai Meirovitch.	12084
Absolute entropy and free energy of fluids using the hypothetical scanning method.	
II. Transition probabilities from canonical Monte Carlo simulations of partial systems	
Ronald P. White and Hagai Meirovitch.	12096
Monte Carlo wave-function approach to the quantum-phase dynamics of a dissipative molecular system interacting with a single-mode amplitude-squeezed field	
Masayoshi Nakano, Ryohei Kishi, Tomoshige Nitta, and Kizashi Yamaguchi.	12106
Heat capacity estimators for random series path-integral methods by finite-difference schemes	
Cristian Predescu, Dubravko Sabo, J. D. Doll, and David L. Freeman.	12119
Comparative assessment of a new nonempirical density functional:	
Molecules and hydrogen-bonded complexes	
Viktor N. Staroverov, Gustavo E. Scuseria, Jianmin Tao, and John P. Perdew.	12129
Core-hole Hamiltonians and corrected equivalent core model for systems with equivalent atoms	
Nikolai V. Kryzhevoi, Nickolay V. Dobrodey, and Lorenz S. Cederbaum.	12138
Similarity transformed semiclassical dynamics	
Troy Van Voorhis and Eric J. Heller.	12153
A nonequilibrium Monte Carlo approach to potential refinement in inverse problems	
Nigel B. Wilding.	12163
The Kramers' restricted complete active space self-consistent-field method for two-component molecular spinors and relativistic effective core potentials including spin–orbit interactions	
Yong Seok Kim and Yoon Sup Lee.	12169

(Continued)

Practical evaluation of condensed phase quantum correlation functions: A Feynman–Kleinert variational linearized path integral method	
Jens Aage Poulsen, Gunnar Nyman, and Peter J. Rossky.....	12179
Self-consistent density matrix algorithm for electronic structure and excitations of molecules and aggregates	
Shaul Mukamel and Oleg Berman.....	12194
A fast-Fourier transform method to solve continuum-electrostatics problems with truncated electrostatic interactions: Algorithm and application to ionic solvation and ion–ion interaction	
Christine Peter, Wilfred F. van Gunsteren, and Philippe H. Hünenberger.....	12205
 Gas Phase Dynamics and Structure: Spectroscopy, Molecular Interactions, Scattering, and Photochemistry	
Electron rescattering and the dissociative ionization of alcohols in intense laser light	
F. A. Rajgara, M. Krishnamurthy, and D. Mathur.....	12224
Theoretical calculations of the Xe chemical shifts in cryptophane cages	
Devin N. Sears and Cynthia J. Jameson.....	12231
Laser spectroscopy of Nil: Ground and low-lying electronic states	
W. S. Tam, J. W.-H. Leung, Shui-Ming Hu, and A. S.-C. Cheung.....	12245
Density and binding forces: Rotational barrier of ethane	
J. Fernández Rico, R. López, I. Ema, and G. Ramírez.....	12251
A comparative study of electron and positron scattering from chlorobenzene (C₆H₅Cl) and chloropentafluorobenzene (C₆F₅Cl) molecules	
C. Makoche Kanwa, O. Sueoka, and M. Kimura.....	12257
Collision-induced absorption in the rototranslational band of dense hydrogen gas	
Magnus Gustafsson, Lothar Frommhold, Denise Bailly, Jean-Pierre Bouanich, and Claude Brodbeck.....	12264
A systematic <i>ab initio</i> study of the structure and vibrational spectroscopy of HgCl₂, HgBr₂, and HgBrCl	
Nikolai B. Balabanov and Kirk A. Peterson.....	12271
Kohn–Sham density-functional study of the adsorption of acetylene and vinylidene on iron clusters, Fe_n/Fe_n⁺ (n=1–4)	
Steeve Chrétien and Dennis R. Salahub.....	12279
Kohn–Sham density-functional study of the formation of benzene from acetylene on iron clusters, Fe/Fe_n⁺ (n=1–4)	
Steeve Chrétien and Dennis R. Salahub.....	12291
Finite temperature behavior of impurity doped Lithium cluster, Li₆Sn	
Kavita Joshi and D. G. Kanhere.....	12301
Dynamics of electronic excitation in collisions of alkali atoms with noble-gas atoms using atomic core potentials	
A. Reyes and D. A. Micha.....	12308
Dynamics of spin–orbit recoupling in collisions of alkali atoms with noble-gas atoms using atomic core potentials	
A. Reyes and D. A. Micha.....	12316
A theoretical investigation of valence and Rydberg electronic states of acrolein	
Francesco Aquilante, Vincenzo Barone, and Björn O. Roos.....	12323
Highly predissociative levels of CH₃S (A²A₁) detected with degenerate four-wave mixing	
Chin-Ping Liu, Yoshiyuki Matsuda, and Yuan-Pern Lee.....	12335
Autoionization in I and I₂ observed by multiphoton ionization and photoelectron spectroscopy: Two atomic iodine Rydberg series built on the ...5s²5p⁴³P₁ ion core and revised value for the I⁺(³P₁) limit	
Y.-Y. Gu, A. M. Chojnacki, C. J. Zietkiewicz, A. A. Senin, and J. G. Eden.....	12342
One-photon mass-analyzed threshold ionization spectroscopy of 2-bromopropene (2-C₃H₅Br): Analysis of vibration and internal rotation in the cation	
Mina Lee and Myung Soo Kim.....	12351
Theoretical studies of intersystem crossing effects in the O(³P, ¹D)+H₂ reaction	
Biswajit Maiti and George C. Schatz.....	12360

Condensed Phase Dynamics, Structure, and Thermodynamics: Spectroscopy, Reactions, and Relaxation

Cross-relaxation between macromolecular and solvent spins: The role of long-range dipole couplings Bertil Halle.....	12372
<i>Ab initio</i> molecular dynamics study of polarization effects on ionic hydration in aqueous AlCl₃ solution Takashi Ikeda, Masaru Hirata, and Takaumi Kimura.....	12386
Mechanism of unidirectional motions of chiral molecular motors driven by linearly polarized pulses Kunihito Hoki, Masahiro Yamaki, Shiro Koseki, and Yuichi Fujimura.....	12393
Fast relaxation in the structural glass and glassy crystal of ethanol and cyano cyclohexane: A quasielastic light scattering study N. V. Surovtsev, S. V. Adichtchev, J. Wiedersich, V. N. Novikov, and E. A. Rössler.....	12399
Stationary points and dynamics in high-dimensional systems David J. Wales and Jonathan P. K. Doye.....	12409
Time dependent density functional theory study of charge-transfer and intramolecular electronic excitations in acetone–water systems Leonardo Bernasconi, Michiel Sprik, and Jürg Hutter.....	12417
Near-infrared spectroscopic study of water at high temperatures and pressures Yusuke Jin and Shun-ichi Ikawa.....	12432
Departures from the correlation of time- and temperature-dependences of the α-relaxation in molecular glass-formers C. M. Roland, M. Paluch, and S. J. Rzoska.....	12439
Application of database methods to the prediction of B3LYP-optimized polyhedral water cluster geometries and electronic energies David J. Anick.....	12442
Influence of ions on the hydrogen-bond structure in liquid water Anne Willem Omta, Michel F. Kropman, Sander Woutersen, and Huib J. Bakker.....	12457

Surfaces, Interfaces, and Materials

Excited-state charge transfer dynamics in systems of aromatic adsorbates on TiO₂ studied with resonant core techniques J. Schnadt, J. N. O'Shea, L. Patthey, L. Kjeldgaard, J. Åhlund, K. Nilson, J. Schiessling, J. Krempaský, M. Shi, O. Karis, C. Glover, H. Siegbahn, N. Mårtensson, and P. A. Brühwiler.....	12462
Equilibration in two chambers connected by a capillary Leonardo Dagdug, Alexander M. Berezhkovskii, Stanislav Y. Shvartsman, and George H. Weiss.....	12473
A cunning strategy in design of polymeric nanomaterials with novel microstructures Lei Huang, Xuehao He, Tianbai He, and Haojun Liang.....	12479
Asymptotic relations between time-lag and higher moments of transient nucleation flux Vitaly A. Shneidman.....	12487
Effect of a static electric field on the vibrational and electronic properties of a compressed CO adlayer on Pt(110) in nonaqueous electrolyte as probed by infrared reflection–absorption spectroscopy and infrared-visible sum-frequency generation spectroscopy F. Vidal, B. Busson, A. Tadjeddine, and A. Peremans.....	12492
Structural quantum isotope effects in amorphous beryllium hydride Sujatha Sampath, Kristina M. Lantzky, Chris J. Benmore, Jörg Neuefeind, Joan E. Siewenie, Peter A. Egelstaff, and Jeffery L. Yarger.....	12499
Core level spectroscopy and reactivity of coadsorbed K+O layers on reconstructed Rh(110) surfaces S. Günther, H. Marbach, R. Imbihl, A. Baraldi, S. Lizzit, and M. Kiskinova.....	12503
A new methodology and model for characterization of nucleation and growth kinetics in solids D. J. Safarik and C. B. Mullins.....	12510
NO adsorption on Rh(100). I. Structural characterization of the adlayers F. Bondino, G. Comelli, A. Baraldi, E. Vesselli, R. Rosei, A. Goldoni, S. Lizzit, C. Bungaro, S. de Gironcoli, and S. Baroni.....	12525
NO adsorption on Rh(100). II. Stability of the adlayers F. Bondino, G. Comelli, A. Baraldi, E. Vesselli, R. Rosei, A. Goldoni, and S. Lizzit.....	12534

(Continued)

Structure and dynamics of liquid water adsorbed on the external walls of carbon nanotubes J. Martí and M. C. Gordillo.....	12540
C₆₀ bonding to graphite and boron nitride surfaces P. Reinke, H. Feldermann, and P. Oelhafen.....	12547
Rotational effects in dissociation of H₂ on Pd(111): Quantum and classical study H. F. Busnengo, E. Pijper, G. J. Kroes, and A. Salin.....	12553
Effect of an external electric field on the charge transport parameters in organic molecular semiconductors J. C. Sancho-García, G. Horowitz, J. L. Brédas, and J. Cornil.....	12563
Molecular-dynamics simulations of the ethanol liquid–vapor interface Ramona S. Taylor and Roseanne L. Shields.....	12569
Hydrogen bonding between adsorbed deprotonated glycine molecules on Cu(110) M. Nyberg, M. Odelius, A. Nilsson, and L. G. M. Pettersson.....	12577
The effect of discrete attractive fluid–wall interaction potentials on adsorption isotherms of Lennard-Jones fluid in cylindrical pores Xianren Zhang, Dapeng Cao, and Wenchuan Wang.....	12586
Examination of liquid metal surfaces through angular and energy measurements of inert gas collisions with liquid Ga, In, and Bi Michelle Manning, Jason A. Morgan, David J. Castro, and Gilbert M. Nathanson.....	12593
Formation of neutral and charged gold carbonyls on highly faceted gold nanostructures Thoi-Dai Chau, Thierry Visart de Bocarmé, Norbert Kruse, Richard L. C. Wang, and Hans Jürgen Kreuzer.....	12605
Density-functional theory for polar fluids at functionalized surfaces. I. Fluid-wall association Sandeep Tripathi and Walter G. Chapman.....	12611

Polymers, Biopolymers, and Complex Systems

Structure of polyelectrolytes in 3:1 salt solutions J. M. G. Sarraguça, M. Skepö, A. A. C. C. Pais, and P. Linse.....	12621
Depletion interactions induced by flexible polymers in solutions of rod-like macromolecules Xiaoling Wang and Avik P. Chatterjee.....	12629
Adsorption of rod-like polyelectrolytes onto weakly charged surfaces Hao Cheng and Monica Olvera de la Cruz.....	12635
Lattice model of equilibrium polymerization. IV. Influence of activation, chemical initiation, chain scission and fusion, and chain stiffness on polymerization and phase separation Jacek Dudowicz, Karl F. Freed, and Jack F. Douglas.....	12645
Effect of polymer–polymer interactions on the surface tension of colloid–polymer mixtures A. Moncho-Jordá, B. Rotenberg, and A. A. Louis.....	12667
Anomalous diffusion of vibrational energy in proteins Xin Yu and David M. Leitner.....	12673

LETTERS TO THE EDITOR

Notes

Comment on “Strontium clusters: Many-body potential, energetics, and structural transitions” [J. Chem. Phys. 115, 3640 (2001)] Jonathan P. K. Doye and Florent Calvo.....	12680
---	-------

Errata

Erratum: Six-dimensional variational calculation of the bending energy levels of HF trimer and DF trimer [J. Chem. Phys. 115, 9781 (2001)] Xiao-Gang Wang and Tucker Carrington Jr.....	12682
Cumulative Author Index.....	12683

***Ab initio* molecular dynamics study of polarization effects on ionic hydration in aqueous AlCl_3 solution**

Takashi Ikeda,^{a)} Masaru Hirata, and Takaumi Kimura

Department of Materials Science, Japan Atomic Energy Research Institute (JAERI), Tokai-mura, Naka-gun, Ibaraki 319-1195, Japan

(Received 2 September 2003; accepted 25 September 2003)

The solvation shell structure and dynamics of Al^{3+} and Cl^- in an aqueous solution of 0.8 M AlCl_3 are studied under ambient conditions by using an *ab initio* molecular dynamics method. The solvation structures obtained from our *ab initio* simulations are in good agreement with the experimental ones for both Al^{3+} and Cl^- . A detailed analysis of intramolecular geometry of hydration waters and dipole moments of the ingredients shows that the polarization has substantial effects on the structures and dynamics of both the cation and anion hydration shells. Implications for metal hydrolysis of Al^{3+} will also be given. © 2003 American Institute of Physics.

[DOI: 10.1063/1.1627323]

I. INTRODUCTION

The aqueous solvation of ions is the initial step of many processes occurring in solution. It is thus of prime interest in a variety of fields ranging from physics to biology. Indeed, the solvation structure and dynamics of ions in water play an important role in many chemical processes. An example of such processes is the complex formation reaction; it only proceeds after the dehydration of ions takes place. To many biological processes, the hydration structure of ions and its dynamics are also of vital importance. The selectivity of biological ion channels is a good representative of showing that biological systems mostly acquire their functions via the hydration process.

The aluminum ion Al^{3+} is one of the most abundant metal ions in natural waters. Its concentration in seawater amounts to 7.9×10^{-8} M.¹ The aquatic chemistry of Al^{3+} still remains a subject of fundamental interest after many years of intensive research. The Al^{3+} ion in acidic solutions is known to exist as a six-fold coordinated ion, conventionally denoted by $[\text{Al}(\text{H}_2\text{O})_6]^{3+}$, where six water molecules are octahedrally arranged around Al^{3+} .² The ion–water interactions in this hexahydrate ion are so strong that the rate of the water exchange reaction never exceeds 10 s^{-1} . This enables us to estimate the coordination number of Al^{3+} using ^{17}O nuclear magnetic resonance (NMR) experiment³ for AlCl_3 in H_2 ^{17}O water.

Within the *pH* range of natural waters, however, the aluminum ion is already coordinated with OH^- ions because the hexahydrate undergoes the hydrolysis reactions producing various hydroxo complexes. Whereas the speciation, thermodynamics, and transformation mechanisms of these hydrolysis products are still a matter of debate, many practical applications of aluminum hydrolysis products were also found recently, ranging from pharmaceutical design⁴ to purification of water.⁵ Since aluminum is the most abundant metal in the Earth's crust, the potential of aluminum hydroly-

sis products should be pursued further for practical applications.

The hydration of anions is usually much weaker than that of multiply charged cations except for limited cases, such as OH^- and F^- .² Thus, the information on the hydration structure of anions is not very conclusive compared to that of the cations, despite the fact that a large number of experiments have already been carried out for this purpose. Among anions, the chloride ion Cl^- was most extensively investigated both experimentally and theoretically. Despite much effort, detailed information on the hydration structure of Cl^- is still hardly obtained experimentally. This could be attributed to the dynamic properties particular to water molecules around Cl^- ; the rotational correlation time of water molecules around Cl^- is even smaller than that of bulk water.⁶

However, Kropman and Bakker⁷ directly measured the dynamics of water molecules in the solvation shells of Cl^- , Br^- , and I^- with femtosecond midinfrared nonlinear spectroscopy. This nonlinear technique enables the clear distinction between the spectral response of the water molecules in the solvation shell and that of the other water molecules in the solution. They found that the water molecules in the solvation shells of these anions move comparatively slowly. The mean lifetimes estimated with an uncertainty of about 5 ps range from 12 to 20 ps for 1–6 M NaCl solutions and 18–25 ps for NaBr and NaI in the same range of concentrations.

The solvation structures of strong electrolyte aqueous solutions are usually described in terms of independent hydrated ions. In fact, this description of the electrolyte solutions is commonly used for analysis of various experimental results and for thermodynamic arguments of these solutions as well. However, the use of the hypothesis of independent hydrated ions raises serious questions for highly concentrated solutions; even though metal cations are not directly coordinated with anions, hydration shells cannot be completed without some water molecules being shared presum-

^{a)}Electronic mail: tiked@popx.tokai.jaeri

ably between cations and anions. As a result, each hydration shell is expected to be stabilized because additional weak electrostatic interactions act on hydrated ions. Even at low concentrations, anions are not merely an agent for neutralizing the system but sometimes participate themselves in chemical reactions occurring around metal cations. It is, therefore, much desirable that both metal cations and anions are treated on the same footing in the theoretical studies, even for the hydration structure and dynamics of ions in solutions.

In the present article, we report on a theoretical study of aqueous AlCl_3 solution at 0.8 M. Our computational approach is based on the *ab initio* molecular dynamics method⁸ applied in previous studies of hydration structure of ions, such as Li^+ ,⁹ Be^{2+} ,¹⁰ Na^+ ,¹¹ Mg^{2+} ,¹² K^+ ,¹³ Ca^{2+} ,¹⁴ and Ag^+ (Ref. 11) for metal ions and Br^- (Ref. 15) for anions. The major advantage of this method is that it does not rely on fitted force fields but determines the forces acting on each atom from first principles on the fly. This is a requisite for many systems including our solution for which reliable force fields are scarcely obtained *a priori*. Our primary aim is to construct a realistic model of an aqueous AlCl_3 solution as an example of the systems containing trivalent cations. These cations in solution activate water molecules in many cases, thereby a couple of interesting phenomena are frequently observed, such as hydrolysis reaction, polynuclear complex formation, etc.

The article is organized as follows. In Sec. II, we describe the *ab initio* method and details of the simulations. In Sec. III, we present the results of the simulations and detailed analysis of structural, dynamical, and electronic properties. In Sec. IV, we draw some conclusions.

II. METHODS

We performed Car–Parrinello⁸ molecular dynamics simulations of an aqueous AlCl_3 solution using first-principles techniques within the Hamprecht–Cohen–Tozer–Handy¹⁶ gradient corrected density functional theory. It has been demonstrated¹⁷ that this exchange–correlation functionals describes more satisfactorily the hydrogen bond and transport properties of liquid water than the very popular Becke¹⁸ and Lee–Yang–Parr¹⁹ exchange and correlation functions. The valence–core interaction was described by norm-conserving Troullier–Martins pseudopotentials²⁰ for all atoms except for hydrogen for which a von Barth–Car analytical pseudopotential²¹ was used. Valence orbitals were expanded in a plane-wave basis set with an energy cutoff of 70 Ry and periodic boundary conditions on the simulation cell were applied. The Brillouin zone of the cell was sampled at the Γ point only. The equations of motion were integrated with a time step of 7 a.u. (0.169 fs) using a fictitious electron mass of 1000 a.u. All of the hydrogen atoms were replaced by deuterium.

The simulation of an aqueous AlCl_3 solution was started from a configuration of normal liquid water consisting of 64 water molecules in a cubic box of side $L = 12.857 \text{ \AA}$. To generate an initial configuration of an aqueous AlCl_3 solution, four water molecules were replaced by solute ions, i.e., one Al^{3+} and three Cl^- ions. Then extra two water mol-

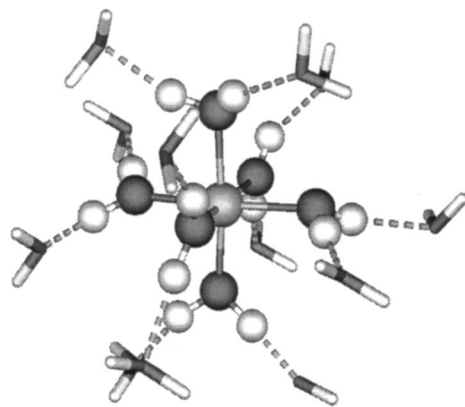


FIG. 1. A snapshot of the hydrated aluminum ion $[\text{Al}(\text{D}_2\text{O})_6]^{3+}$ taken from our *ab initio* molecular dynamics simulations for aqueous AlCl_3 solution. Water molecules in the second shell are represented using cylinder models. Hydrogen bonds are indicated by dashed lines.

ecules were added to take account of the negative solvation volume of Al^{3+} in water. Our sample, thus generated, is an aqueous AlCl_3 solution at 0.8 M. After heating the system to a temperature of 600 K for ~ 5 ps, it was cooled down to 300 K over a period of ~ 2 ps. The trajectories were collected for 28 ps under constant energy conditions after the re-equilibration of the system for ~ 5 ps by the rescaling of the ionic velocities. All of the simulations were performed using the CPMD package.²²

III. RESULTS AND DISCUSSION

A. Overview

According to the analysis of the stability constants of metal–ligand complexes in aqueous solutions by Ahrland *et al.*²³ and Schwarzenbach,²⁴ there is an evident classification of the metal ions into “hard” and “soft” types. The Al^{3+} ion has the electron configuration of the rare gas (Ne) characteristic of hard sphere cations. Metal cations of the hard type are well known to form complexes preferentially with ligands having oxygen as the donor atom. In fact, as shown in Fig. 1, a hydrated aluminum ion conventionally denoted by $[\text{Al}(\text{D}_2\text{O})_6]^{3+}$ was formed as soon as the simulation was started, though our sample also contains three Cl^- ions. The Cl^- anions are separated from an Al^{3+} cation by two or more water molecules; Cl^- ions have their own solvation shells as will be shown later.

The Al^{3+} ion is tightly bound to hydration water molecules, thereby the diffusive motion of Al^{3+} was hardly observed in our molecular dynamics simulation of 28 ps length as shown in Fig. 2. On the other hand, the Cl^- anions show rather large diffusivity comparable to the bulk water irrespective of a heavier mass than a deuterated water molecule. Consequently, the Cl^- ions sometimes approach the outer sphere of the hydrated Al^{3+} ion and one or two hydration water molecules are thus temporarily shared with the Al^{3+} and Cl^- solvation shells.

Although our aqueous solution does not contain any explicit inhibitors of hydrolysis reactions, such as HCl , we

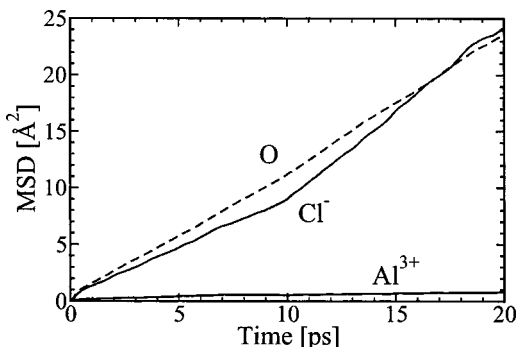


FIG. 2. Mean-square displacement of Al^{3+} , Cl^- , and oxygen atoms of the bulk waters as a function of time in aqueous AlCl_3 solution.

could not observe any events of the metal hydrolysis. The implication of our molecular dynamic simulations for metal hydrolysis are present in Sec. IV.

B. Aluminum ion

Further information on the solvation shell structures of Al^{3+} is obtainable from radial distribution functions (RDFs) $g(r)$ which can be computed directly from our trajectories. The first peak located at 1.92 Å in $g_{\text{AlO}}(r)$ shown in Fig. 3(a) compares well with the experimental one at 1.90 Å determined from x-ray diffraction for 1.0 M AlCl_3 .²⁵ The second peak at 4.09 Å in $g_{\text{AlO}}(r)$, well separated from the first peak, has a rather large full width at half maximum of 0.4 Å. Nonetheless, a plateau is still recognizable at ~ 4.8 Å in the oxygen running coordination number for Al^{3+} ; the running coordination number at 4.8 Å is obtained as 18.0 unambiguously. Comparing $g_{\text{AlO}}(r)$ [Fig. 3(a)] and $g_{\text{AlD}}(r)$ [Fig. 3(b)], we find that the deuterium atoms of the hydration waters in

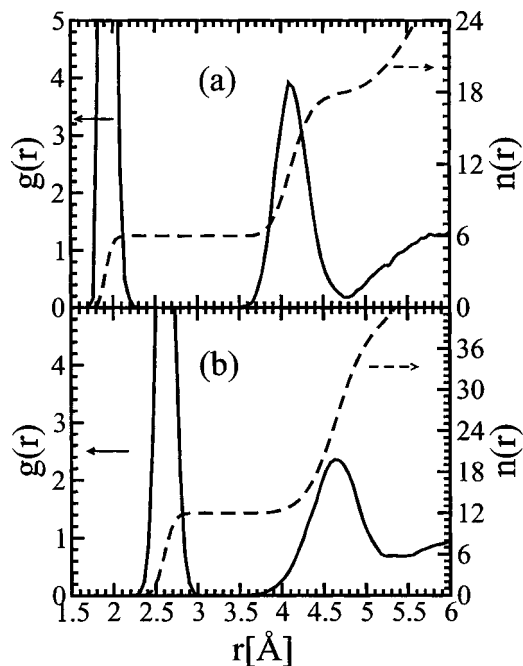


FIG. 3. Radial distribution functions (a) $g_{\text{AlO}}(r)$ and (b) $g_{\text{AlD}}(r)$ for aqueous AlCl_3 solution. The dashed lines represent the running coordination number $n(r)$.

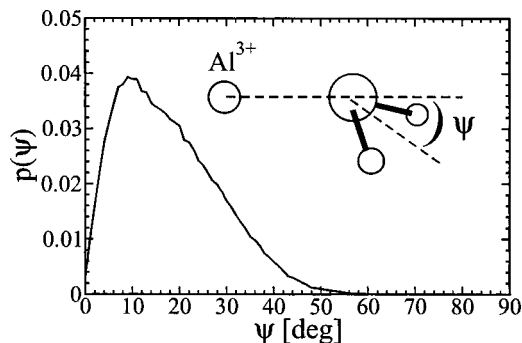


FIG. 4. Distribution of the tilt angle ψ between the dipole moment of the D_2O and the Al^{3+} -O axis within the first solvation shell of Al^{3+} .

the first shell point away from Al^{3+} toward bulk water. In this orientation, the water molecules readily act as hydrogen bond donors. Therefore, each of the 6 water molecules in the first solvation shell of Al^{3+} forms hydrogen bond with 2 water molecules resulting in the formation of the second solvation shell containing 12 water molecules in total as shown in Fig. 1.

The first solvation shell of Al^{3+} containing six D_2O is very well defined; the probability distribution of O- Al^{3+} -O angles within this first shell exhibits two sharp peaks at 90.8° and 174.8° , indicating that six water molecules are octahedrally arranged rather rigidly around Al^{3+} . Although the relative positions of O atoms in the first shell of Al^{3+} are virtually fixed, molecular orientations of the hydration waters show large fluctuations which can be quantified by the distribution of the tilt angle ψ between the dipole moment of the D_2O and the Al^{3+} -O axis. As shown in Fig. 4, the tilt angle ψ is distributed from 0° to 50° and, hence, the estimated average value is $\psi = 18^\circ$ with a standard deviation of 10° . This tilting of the D_2O dipole with respect to the Al^{3+} -O axis arises not only from thermal fluctuations of molecular orientations but also from the fact that the coordination bonds between Al^{3+} and hydration waters are formed through one lone pair orbital of each water molecule as will be shown later.

The Al^{3+} ion is inert in the sense that the water exchange reaction is slow (rate constant $\sim 1 \text{ s}^{-1}$) due to the strong ion-water interactions.² Indeed, these strong interactions lead to the splitting of ^{17}O NMR signals³ observed in H_2^{17}O water; one signal comes from bulk water in the lower field while another one comes from hydration waters in the higher field giving an estimate of the coordination number of Al^{3+} as 6 from the area under the peak. Consistent with the ^{17}O NMR measurement, the analysis of molecular structures of D_2O clarifies that the six water molecules in the first shell are distinguishable from the others; as shown in Fig. 5(a) the O-D bond length of 6 D_2O in the first shell is 0.02 Å longer on average than that of other water molecules in the solution. In addition, the D-O-D angle of the hydration waters is also large by about 2° on average compared to that of the other water molecules as shown in Fig. 5(b).

More remarkable is that the molecular dipole moment μ of hydration waters of Al^{3+} is greatly enhanced particularly for six waters in the first shell. While the distribution of μ

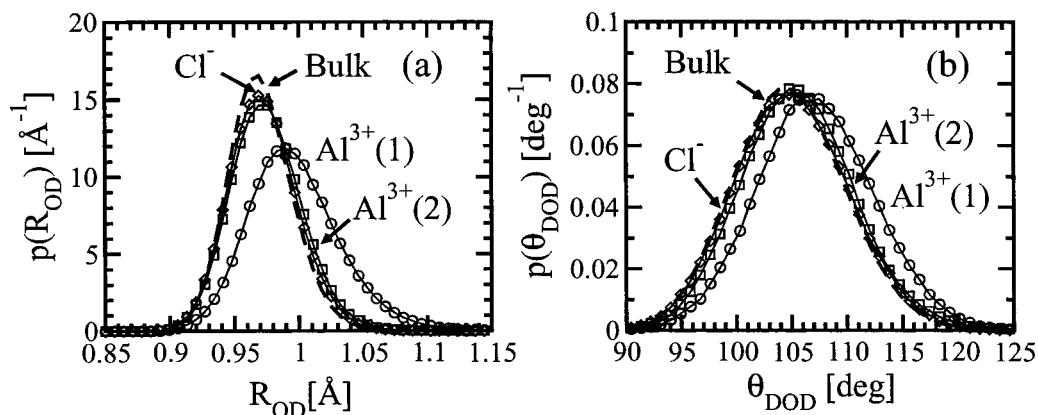


FIG. 5. The distribution of (a) the O-D bond length and (b) the D-O-D bond angle of water molecules in aqueous AlCl_3 solution. Open circles, squares, and diamonds give the distributions concerned with water molecules in the first $[\text{Al}^{3+}(1)]$ and second $[\text{Al}^{3+}(2)]$ shells of Al^{3+} , and in the solvation shell of Cl^- , respectively. The corresponding distributions for the bulk are shown by dashed lines.

calculated from maximally localized Wannier function centers (WFCs) for hydration waters is as broad as that in normal liquid water,²⁶ the maximum is centered at 4.14 ± 0.29 and 3.02 ± 0.28 D for water molecules in the first and second shells of Al^{3+} , respectively (Fig. 6). The distribution for the other water molecules in the solution is almost the same as that in the bulk; the maximum is centered at 2.83 ± 0.28 D in agreement with the theoretical results for normal liquid water.^{12,15,26} The great enhancement of molecular dipole moment of waters directly coordinating an Al^{3+} ion is due mainly to the redistribution of the electrons induced by strong electric field of Al^{3+} . The contribution of the nuclear charge is minor though the O-D bonds are elongated by as much as 0.02 \AA .

Figure 7 shows the distribution of the distance between the oxygen and WFCs for hydration waters in the first solvation shell of Al^{3+} and in the bulk. For a water molecule, there are four doubly occupied Wannier functions (WFs) per molecule in the pseudopotential approach. Two of the WFs correspond to the O-D(H) covalent bonds while the remaining two WFs correspond to the lone-pair orbitals on the oxygen atom. In ambient water, the center of these WFs is located at ~ 0.50 and ~ 0.32 \AA away from the oxygen atom for

the covalent bonds and lone-pair orbitals, respectively. The two lone-pair orbitals of hydration waters are no more equivalent in the first shell of Al^{3+} because only one lone-pair orbital is involved in the formation of the hydrated ion. This reflects clearly in the difference of the O-WFC distance; the lone-pair orbital involved in the coordination bond between an Al^{3+} ion and a hydration water is pulled by the acceptor atom more strongly than in hydrogen bond O-D \cdots O occurring in ambient water, elongating the O-WFC distance by as much as 0.08 \AA . On the other hand, the remaining lone-pair orbital is contracted by 0.03 \AA compared to that in the bulk because it is virtually free from any coordination bond including hydrogen bond. Therefore, the shift of the peaks with respect to those in the bulk for the lone-pair orbitals in the distribution of the O-WFC distance is an indicator of the strength of the ion-water interactions as well as hydrogen bond in the bulk. In fact, the shift for the lone-pair orbitals involved in the ion-water complexation of Al^{3+} is more pronounced than that of Mg^{2+} examined in Ref. 12.

In addition to the clear distinction between the two lone-pair orbitals, we find that the WFCs associated with the O-D covalent bonds come closer to the oxygen atom by about 0.02 \AA . Recall that the WFCs corresponding to the O-D

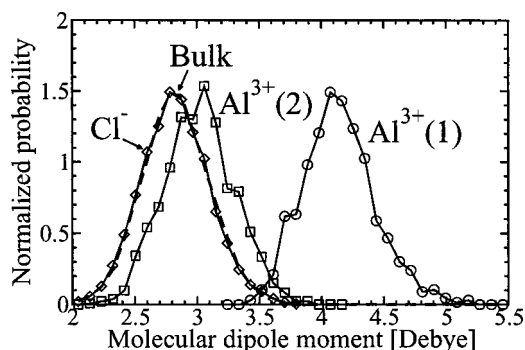


FIG. 6. The distribution of molecular dipole moments of waters calculated from maximally localized WFCs. Open circles, squares, and diamonds give the distributions concerned with water molecules in the first $[\text{Al}^{3+}(1)]$ and second $[\text{Al}^{3+}(2)]$ shells of Al^{3+} , and in the solvation shell of Cl^- , respectively. The corresponding distributions for the bulk are shown by dashed lines.

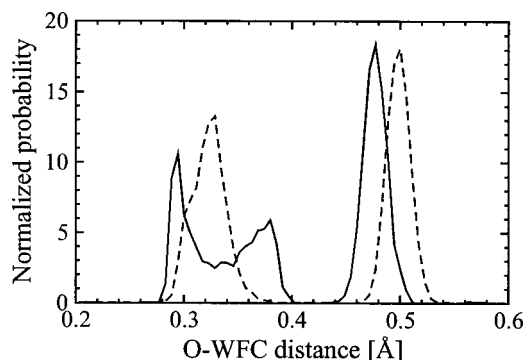


FIG. 7. The distribution of the O-WFC distance for the water molecules in the first solvation shell of Al^{3+} (solid lines) and in the bulk (dashed lines). The peaks located between 0.28 \AA and 0.4 \AA correspond to the lone-pair orbitals while the remaining peaks around 0.5 \AA correspond to the O-D covalent bonds.

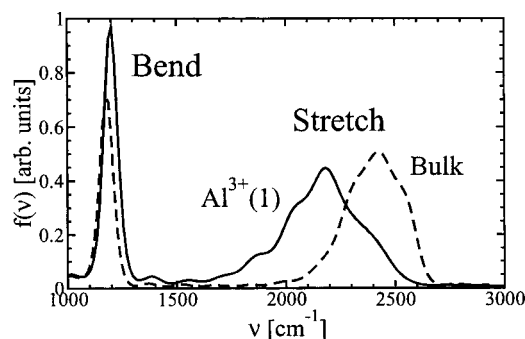


FIG. 8. Vibrational density of states in the bending and stretching mode region of D_2O in the first solvation shell of Al^{3+} (solid line) and in the bulk (dashed line) obtained from the velocity autocorrelation functions.

covalent bonds in the bulk reside at almost the midpoint between the oxygen and deuterium atoms, their shift toward the O atom thus indicates that the covalency of the O–D bonds is reduced substantially. Therefore, this charge redistribution weakens the O–D bonds, manifesting itself in the redshift of $\sim 250\text{ cm}^{-1}$ in the O–D stretching mode frequency estimated from the velocity autocorrelation functions (Fig. 8).

C. Chloride ion

In the solvation shell of a Cl^- ion, deuterium (hydrogen) of hydration waters works as the acceptor meaning that one of the O–D(H) bonds points to a chloride ion, leading to the linear O–D $\cdots Cl^-$ hydrogen bond. The formation of this linear hydrogen bond in the aqueous solutions was confirmed by neutron diffraction experiment.²⁷ Its high directionality was also revealed from our molecular dynamics simulations by calculating the distribution of the tilt angle θ between the $Cl^- \cdots D$ and $Cl^- - O$ axes ($\theta = 6 \pm 4^\circ$).

Whereas the coordination number of Cl^- obtained by integrating the RDF $g_{ClO}(r)$ [Fig. 9(a)] up to its first minimum is 6.03 which is in good agreement with the experimental result (5.8 ± 0.5) for aqueous LiCl solution,²⁷ the two features of the RDFs, namely, the nonzero first minimum of $g_{ClO}(r)$ and the vanishing of structures in $g_{ClD}(r)$ at $r > 4.0\text{ \AA}$ [Fig. 9(b)] suggest that the hydration waters are exchanged with bulk waters rather rapidly. Indeed, as shown in Fig. 10, the instantaneous coordination number defined as the number of oxygen atoms closer than 3.85 \AA to the Cl^- ion is distributed from 4.0 to 8.0 with an average number being 5.9 ± 0.8 .

As opposed to the hydration of Al^{3+} , the intramolecular structures and the dipole moment of hydration waters for Cl^- are found to be almost identical to those of bulk waters (Figs. 5 and 6). This does not come as a surprise when we notice that the lone-pair orbitals of the hydration waters, which respond very sensitively to the presence of the acceptor atom as demonstrated in Fig. 7, point not to Cl^- ions but to the bulk. Therefore, in this orientation, the hydration waters appear to be hardly influenced by coordinating a Cl^- ion. However, Kropman, and Bakker⁷ show that the hydrogen bond dynamics of water molecules solvating a halogenic anion is slow compared to neat liquid water using femtosec-

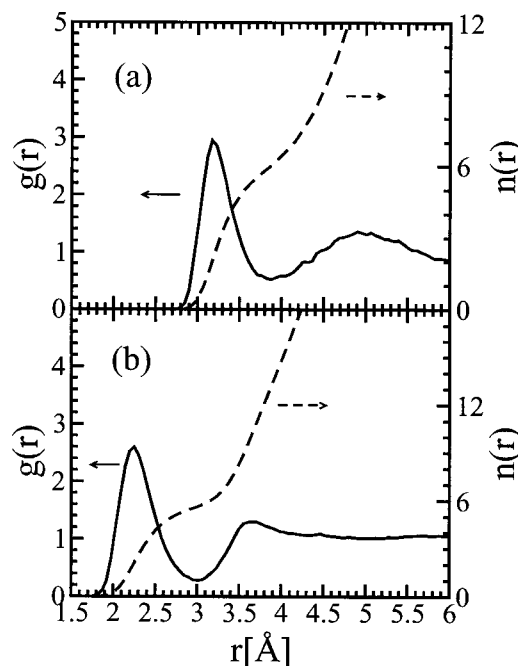


FIG. 9. Radial distribution functions (a) $g_{ClO}(r)$ and (b) $g_{ClD}(r)$ for aqueous $AlCl_3$ solution. The dashed lines represent the running coordination number $n(r)$.

ond midinfrared nonlinear spectroscopy. According to Kropman and Bakker,⁷ the residence time τ of water molecules in the first solvation shell of a halogenic anion depends somewhat on the concentrations; increasing the concentration from 1 to 6 M changes τ from 12 ± 4 to 20 ± 5 ps for a solution of NaCl. We have estimated the mean residence time by following the prescription of Impey *et al.*²⁸ where any molecule that does not leave the solvation shell for a time longer than t^* , without returning into it in the interim, is treated as not having left the solvation shell at all. Following former studies^{15,28–31} a tolerance time of $t^* = 2$ ps was used. The computed decay of the population of water molecules in the solvation shell shown in Fig. 11 gives a rough estimate of $\tau \approx 8.8$ ps for our aqueous $AlCl_3$ solution. Although this theoretical value of the mean residence time is somewhat smaller than the experimental one for aqueous

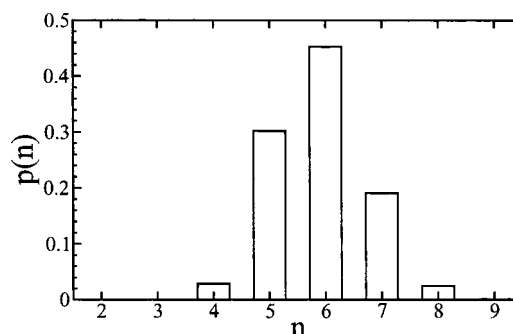


FIG. 10. The distribution of instantaneous coordination number n of Cl^- . The instantaneous coordination number is defined as the number of oxygen atoms closer than 3.85 \AA to the Cl^- ion. The average coordination number of 5.9 ± 0.8 agrees well with the experimental one of 5.8 ± 0.5 (see Ref. 27).

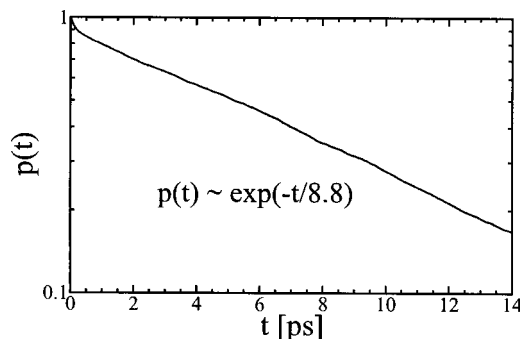


FIG. 11. The decay of the water population of the Cl^- solvation shell. Shown is the probability $p(t)$ that water molecules lying initially within the solvation shell of Cl^- are still there after a time t has elapsed without ever having entered the bulk in the description of Impey *et al.* (Ref. 28).

NaCl solution, it is certainly at least ten times longer than the mean lifetime of the $\text{O}-\text{D}(\text{H})\cdots\text{O}$ hydrogen bond (~ 0.5 ps).

The $\text{O}-\text{D}\cdots\text{Cl}^-$ hydrogen bond in our aqueous solution is definitely strong compared to the usual hydrogen bond $\text{O}-\text{D}\cdots\text{O}$ formed in normal liquid water. Considering that hydration waters of Cl^- are hardly distinguished from bulk waters from the viewpoint of the intramolecular geometry and the molecular dipole moment, the strengthening of the $\text{O}-\text{D}\cdots\text{Cl}^-$ bond is expected to originate from the electronic properties of Cl^- and/or its solvation shell structure itself. Figure 12(a) shows the distribution of dipole moment of Cl^- computed from the WFCs associated with Cl^- . It turns out that the Cl^- ion has an induced net dipole moment; the average value of the anion dipole moment μ is estimated as $\mu = 0.66 \pm 0.3$ D. Since the polarization of anions in solution would be related to the residence time of hydration waters, somewhat smaller dipole moment of Cl^- than that of Br^- in aqueous HBr solution ($\mu \approx 0.95$ D¹⁵) is considered to be consistent with the observed dependence of the residence time on the anions: 12 to 20 ps for 1–6 M NaCl solutions and 18 to 25 ps for NaBr in the same range of concentrations.

In the presence of the net anion dipole moment, the solvation shell of Cl^- itself is likely to be polarized so that the ion–water complex is more stabilized. The ultimate structure along the line is the surface solvation which is known to occur depending on a delicate balance among the stabiliza-

tion of the first solvation shell, the destabilization of the second shell, and longer distance interactions.³² To characterize the asymmetry of the solvation shell of Cl^- , we introduce a vector given by $\mathbf{R}_{\text{cage}} = \sum_{\{i\}} (\mathbf{R}_{\text{O}_i} - \mathbf{R}_{\text{Cl}})$. Here, the sum for the oxygen positions \mathbf{R}_{O_i} is taken over the oxygen atoms in the instantaneous solvation shell of a given chloride ion located at \mathbf{R}_{Cl} . Then, a parameter ϕ defined as $\cos \phi = \frac{\boldsymbol{\mu}_{\text{Cl}} \cdot \mathbf{R}_{\text{cage}}}{|\boldsymbol{\mu}_{\text{Cl}}| |\mathbf{R}_{\text{cage}}|}$ is examined as to whether the correlation exists between a net anion dipole moment $\boldsymbol{\mu}_{\text{Cl}}$ and the asymmetry of solvation shell of Cl^- measured with \mathbf{R}_{cage} . The magnitude of the vector \mathbf{R}_{cage} is found to be substantial ($\langle |\mathbf{R}_{\text{cage}}| \rangle \sim 3.32$ Å) in most of our trajectories, suggesting that the solvation shell of Cl^- is mostly asymmetric as shown in the inset of Fig. 12(b). Moreover, the distribution of angle ϕ shown in Fig. 12(b) is asymmetric with respect to $\phi = 90^\circ$ with an average number of $\langle \cos \phi \rangle = -0.35$. This negative average number indicates that a surfacelike state is formed around Cl^- .³³ Therefore, a net dipole moment of Cl^- is correlated with high probabilities to the formation of asymmetric solvation shell of Cl^- .

IV. CONCLUSIONS

We have performed the *ab initio* molecular dynamics simulations of an aqueous AlCl_3 solution at 0.8 M to study the solvation shell structure and dynamics of Al^{3+} as well as Cl^- . The solvation structure of Al^{3+} in our solution is found to be composed of the two hydration shells: The first shell containing six water molecules arranged octahedrally around Al^{3+} and the second shell of twelve water molecules formed via hydrogen bonds with the six hydration waters in the first shell. The small ionic radius and large charge of Al^{3+} have substantial effects on the charge redistribution of hydration waters in the first shell. This becomes obvious from their anomalously large dipole moment on the one hand and the distinctive intramolecular structures on the other hand. Our analyses based on localized WFs and WFCs describe well these pronounced features of the hydration of Al^{3+} .

In contrast to the well defined solvation structure of Al^{3+} , hydration waters of Cl^- are hardly distinguished from bulk water, though the $\text{O}-\text{D}(\text{H})\cdots\text{Cl}^-$ hydrogen bond is formed. In fact, we found that the hydration waters are ex-

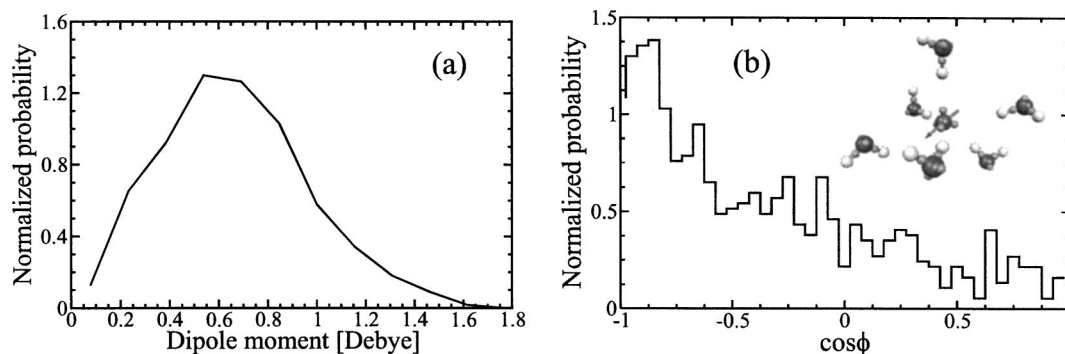


FIG. 12. (a) The distribution of dipole moment of Cl^- and (b) the correlation between an induced net dipole moment of Cl^- and asymmetric structure of its solvation shell. The distribution of the angle ϕ between the direction of the anion dipole moment and the vector defined as $\mathbf{R}_{\text{cage}} = \sum_{\{i\}} (\mathbf{R}_{\text{O}_i} - \mathbf{R}_{\text{Cl}})$ is shown in (b) along with a snapshot of the solvation shell of Cl^- as the inset. Here, the sum for \mathbf{R}_{O_i} is taken over the oxygen atoms in the solvation shell. An arrow and small spheres in the inset indicate the direction of the instantaneous anion dipole moment and WFCs, respectively.

changed with bulk waters at the rate of ~ 9 ps on average. However, this mean lifetime of the $\text{O}-\text{D}\cdots\text{Cl}^-$ bond is certainly longer than that of the $\text{O}-\text{D}\cdots\text{O}$ hydrogen bond in the bulk, indicating that the hydration structure of Cl^- has distinctive features besides high directionality of the $\text{O}-\text{D}\cdots\text{Cl}^-$ bond. Indeed, we found that the Cl^- ions themselves have a rather large net dipole moment and, furthermore, the asymmetric solvation shell is formed with high probabilities around a chloride ion. These two features work cooperatively as evidenced by the correlation between the instantaneous net dipole moment of Cl^- and the asymmetry of its solvation shell structure so as to stabilize a surfacelike state observed in our simulations.

A missing hydrolysis reaction is an apparent drawback of our simulations. The deuterium atoms of hydration waters for Al^{3+} in our solution sometimes came temporarily near to the midpoint between two adjacent oxygen atoms. However, they always persisted in forming neutral D_2O rather than OD^- . Therefore, there must be a missing slow process relevant to the activation of water molecules. Martin³⁴ suggests that the metal hydrolysis of Al^{3+} is accompanied by the decrease of coordination number of Al^{3+} . Such a drastic change of the solvation structure is expected to be a rare event and hardly observed within the time scale accessible by *ab initio* molecular dynamics. Thus, the exploration of the detailed mechanism of metal hydrolysis reactions of Al^{3+} will be the subject of future investigations.

ACKNOWLEDGMENTS

The authors thank Dr. Tsuyoshi Yaita for insightful discussions. The calculations were carried out on HITACHI SR8000-F1 and Fujitsu VPP5000 of JAERI.

¹ See, e.g., W. Stumm and J. J. Morgan, *Aquatic Chemistry*, 3rd ed. (Wiley, New York, 1996).

² H. Ohtaki and T. Radnai, *Chem. Rev.* **93**, 1157 (1993).

³ R. E. Connick and D. N. Fiat, *J. Chem. Phys.* **39**, 1349 (1963).

⁴ W. B. De Almeida, H. F. Dos Santos, and M. C. Zerner, *J. Pharm. Sci.* **87**, 1101 (1998).

⁵ See, e.g., H. May, *Seventh Conference on Water-Rock Interaction* (Balkema, Rotterdam, 1992).

⁶ A. Shimizu and Y. Taniguchi, *Bull. Chem. Soc. Jpn.* **64**, 1613 (1991).

⁷ M. F. Kropman and H. J. Bakker, *Science* **291**, 2118 (2001).

⁸ R. Car and M. Parrinello, *Phys. Rev. Lett.* **55**, 2471 (1985).

⁹ A. P. Lyubartsev, K. Laasonen, and A. Laaksonen, *J. Chem. Phys.* **114**, 3120 (2001).

¹⁰ D. Marx, M. Sprik, and M. Parrinello, *Chem. Phys. Lett.* **373**, 360 (1997).

¹¹ R. Vuilleumier and M. Sprik, *J. Chem. Phys.* **115**, 3454 (2001).

¹² F. C. Lightstone, E. Schwegler, R. Q. Hood, F. Gygi, and G. Galli, *Chem. Phys. Lett.* **343**, 549 (2001).

¹³ L. M. Ramaniah, M. Bernasconi, and M. Parrinello, *J. Chem. Phys.* **111**, 1587 (1999).

¹⁴ M. M. Naor, K. van Nostrand, and C. Dellago, *Chem. Phys. Lett.* **369**, 159 (2003).

¹⁵ S. Rauei and M. L. Klein, *J. Chem. Phys.* **116**, 196 (2002).

¹⁶ F. A. Hamprecht, A. J. Cohen, D. J. Tozer, and N. C. Handy, *J. Chem. Phys.* **109**, 6264 (1998).

¹⁷ A. D. Boese, N. L. Doltsinis, N. C. Handy, and M. Sprik, *J. Chem. Phys.* **112**, 1670 (2000).

¹⁸ A. D. Becke, *Phys. Rev. A* **38**, 3098 (1988).

¹⁹ C. Lee, W. Yang, and R. G. Parr, *Phys. Rev. B* **37**, 785 (1988).

²⁰ N. Troullier and J. L. Martins, *Phys. Rev. B* **43**, 1993 (1991).

²¹ See, e.g., M. Sprik, J. Hutter, and M. Parrinello, *J. Chem. Phys.* **105**, 1142 (1996).

²² CPMD, Copyright IBM Corp 1990-2001, Copyright MPI für Festkörperforschung Stuttgart 1997-2001.

²³ S. Ahrland, S. J. Clatt, and W. R. Davies, *Quart. Rev. London* **12**, 265 (1958).

²⁴ G. Schwarzenbach, *Inorganic Chemistry and Radiochemistry* (Academic, New York, 1961), Vol. 3.

²⁵ R. Caminiti, G. Licheri, G. Piccaluga, G. Pinna, and T. Radnai, *J. Chem. Phys.* **71**, 2473 (1979).

²⁶ P. L. Silvestrelli and M. Parrinello, *Phys. Rev. Lett.* **82**, 3308 (1999).

²⁷ M. Yamagami, H. Wakita, and T. Yamaguchi, *J. Chem. Phys.* **103**, 8174 (1995).

²⁸ R. W. Impey, P. A. Madden, and I. R. McDonald, *J. Phys. Chem.* **87**, 5071 (1983).

²⁹ S. Obst and H. Bradacsek, *J. Phys. Chem.* **100**, 15677 (1996).

³⁰ D. E. Smith and L. X. Dang, *J. Chem. Phys.* **100**, 3757 (1994).

³¹ M. Sprik, M. L. Klein, and K. Watanabe, *J. Phys. Chem.* **94**, 6483 (1990).

³² S. J. Stuart and B. J. Berne, *J. Phys. Chem. A* **103**, 10300 (1999).

³³ The comparable surface state of the chloride complex with water molecules has already been shown to be formed using polarizable force field [L. X. Dang, J. E. Rice, J. Caldwell, and P. A. Kollman, *J. Am. Chem. Soc.* **113**, 2481 (1991)].

³⁴ R. B. Martin, *J. Inorg. Biochem.* **44**, 141 (1991).